C-band 100 Gb/s Transmission over 40 km SSMF Using a Silicon Photonic Vestigial Sideband Transmitter Based on Dual-Drive MZM and Passive Optical Delay Line

Essam Berikaa[1], Md Samiul Alam[1], Yixiang Hu[1], Weijia Li[1], and David V. Plant[1]
[1]*Dept. of Electrical and Computer Engineering, McGill University, Montreal QC H3A 0G4, Canada*
essam.berikaa@mail.mcgill.ca

Abstract: We demonstrate a filter-free silicon photonic VSB transmitter, enabling the C-band transmission of 56 Gbaud PAM4 over 40 km of dispersion-uncompensated SSMF under the 6.7% overhead HD-FEC with a single DAC channel and non-linear equalization.

1. Introduction

Intensity modulation direct detection (IMDD) systems dominate the short-reach datacenter interconnects market because of their cost-effectiveness and simple architecture. However, the transmission reach of IMDD systems is limited by chromatic dispersion (CD) induced power fading, which favors operating IMDD systems in the O-band near the zero-dispersion wavelength. With conventional IMDD architecture and double sideband (DSB) transmission, C-band IMDD systems can not operate beyond 10 km because of the severe power fading at multiple frequencies.

CD-induced power fading can be tackled in the optical domain by employing dispersion compensation fibers (DCF) or creating vestigial sideband (VSB) signals with sharp roll-off optical filters [1]. Alternatively, CD pre-compensation or single sideband (SSB) signaling can mitigate the power fading at the expense of using two DAC channels for complex modulation with either IQ or dual-drive (DD) modulators. These solutions negate the cost-effectiveness and simplicity of IMDD. Yet, the authors in [2] showed that inducing a time skew between differential arms of the DD Mach-Zehnder modulator (MZM) creates a VSB signal. A sinusoidal envelope modulates the DD-MZM output optical signal, yielding a VSB signal for the optimal skew. Previous works employed high-bandwidth tunable RF delay lines for VSB transmission [2,3]; however, incorporating an RF delay line into the IMDD architecture increases cost and complexity.

This paper presents the design and characterization of a C-band silicon photonic (SiP) DD-MZM with an optimized passive optical delay line for VSB generation. We compare the transmission performance of two SiP DD-MZMs, with and without the optical delay line, to quantify the gain of VSB transmission and the effective mitigation of the power fading. Using a single DAC and the delay-based DD-MZM, we transmit a 56 Gbaud PAM4 signal over 40 km of standard single-mode fiber (SSMF) under the 3.8×10^{-3} HD-FEC BER threshold, which corresponds to net 105 Gbps.

2. Modulator Design and Characterization

The cross-sectional view and schematic of the DD-MZMs are presented in Fig. 1(a-b). The chip was fabricated at the Advanced Micro Foundry (AMF) with a standard CMOS-compatible SiP process flow. The DD-MZM is composed of two independent and identical phase shifters connected in parallel. A single differential output DAC drives the two carrier depletion phase shifters, which reduces the driving voltage requirements. Each phase shifter is 4 mm long at a fill factor of 85%. Adding periodic intrinsic regions prevents the flow of electric currents through the optical waveguides. The RF electrodes are designed to match the 50 Ω characteristic impedance of the test equipment and are terminated with an on-chip N^{++} 50 Ω resistor. Vertical grating couplers connect the DD-MZMs optically and have back-to-back (B2B) coupling loss of 11 dB.

The base DD-MZM (without delay) and the DD-MZM with a 10 ps optical delay line show similar characteristics, since they have the same structure and are fabricated on the same chip, as shown in Fig. 1(d). Under 3 V reverse bias, the DD-MZM propagation loss and DC extinction ratio are 5 and 25 dB, respectively. The measured DC $V\pi$ of the individual phase shifter is 6.5 V. Fig. 1(c) shows the frequency response of the base DD-MZM design. The DD-MZM has a 3- (6-) dB bandwidth of 18 (26) GHz at 3 V reverse bias. The modest electro-optic bandwidth of DD-MZMs is attributed to the parallelly connected PN junction capacitances. Yet, the frequency response has a slow roll-off factor enabling operating beyond the 3-dB point. The passive optical delay line is composed of a single spiral waveguide with a total length of 770 μm, which corresponds to a delay of 10 ps for a group index of 3.9. The delay line is designed and optimized for 56 Gbaud transmission; a higher symbol rate requires a shorter delay.

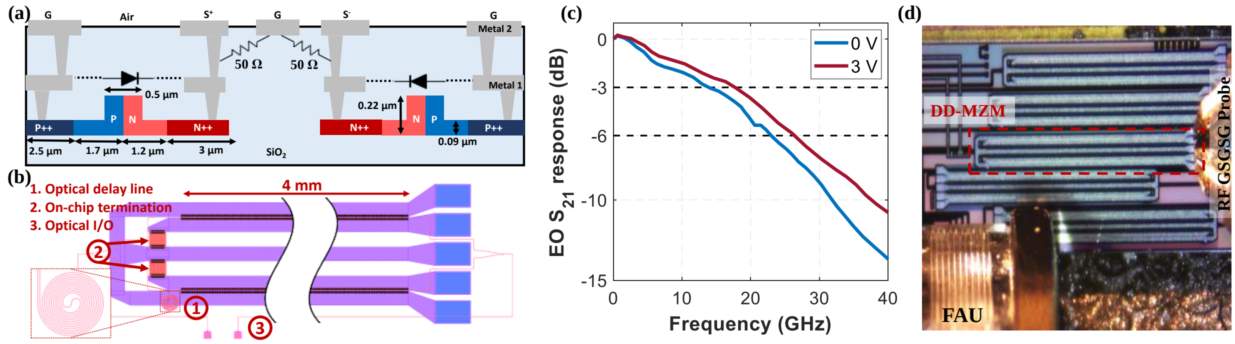

Fig. 1: (a) DD-MZM cross-section (not to scale). (b) DD-MZM layout. (c) The electro-optic (EO) S_{21} response normalized at 1.5 GHz. (d) The fabricated chip showing the optical fiber array unit (FAU) and RF probe (GSGSG).

3. Transmission Experiment

The experimental setup and digital signal processing (DSP) routines are shown in Fig. 2. At the transmitter, the PAM4 symbols are generated from a random binary sequence. The signal is filtered by a raised cosine (RC) pulse shaping filter to limit its bandwidth at 2 samples per symbol (sps) and then resampled to the DAC sampling rate (128 GSa/s). A single pre-emphasis filter is used to pre-compensate for the combined frequency response of the DAC and the driver. The differential outputs of the DAC are amplified by a matched pair of SHF 807c RF drivers (50 GHz bandwidth, 23 dB gain) that drive the DD-MZM via a 50 GHz GSGSG probe. Optically, an external cavity laser (ECL) operating at 1550 nm at 15 dBm feeds the DD-MZM. The inset of Fig. 2 illustrates the difference in the optical spectra between the two tested DD-MZMs, highlighting the impact of the added delay line. After the chip, the signal is amplified by an EDFA to compensate for the grating couplers' loss and then transmitted over various distances of dispersion-uncompensated SSMF. Another EDFA is used after fiber transmission to compensate for the fiber loss, as the receiver does not employ a trans-impedance amplifier (TIA). A variable optical attenuator (VOA) is used to sweep the received optical power (ROP). The output of the 70 GHz photodiode (PD) is digitized by a 256 GSa/s real-time oscilloscope (RTO) for offline DSP processing. The receiver DSP is carried out at 2 sps. For comparison, we considered both linear feed-forward equalizer (FFE) and Volterra non-linear equalizer (VNLE). After equalization, we apply blind geometric distortion to subdue equalization-enhanced noise [4]. Eventually, the recovered symbols are remapped to a bit sequence for BER calculations.

The generated optical spectra of 56 Gbaud PAM4 signals for both DD-MZM structures are shown in Fig. 3(a). The skew induced by the 10 ps optical delay line filters out one sideband, creating a VSB signal. VSB reception reduces the strength of CD-induced power fading and enables longer-reach IMDD transmission in the C-band. Fig. 3(b-d) show the received electrical spectra of 56 Gbaud PAM4 for both DD-MZMs after different fiber lengths. In B2B, the skew induced by the optical delay line effectively filters the high-frequency components of the signal as illustrated in the inset of Fig. 2 and Fig. 3(b). After fiber transmission, the received electrical spectra have strong dips because of the image band and the CD-induced power fading, as shown in Fig. 3(c-d). The DD-MZM with the 10 ps delay has shallower dips because of the VSB nature of the transmitted optical signal, which improves the transmission performance considerably. Yet, the distortion in the received RF spectrum requires strong equalization at the receiver.

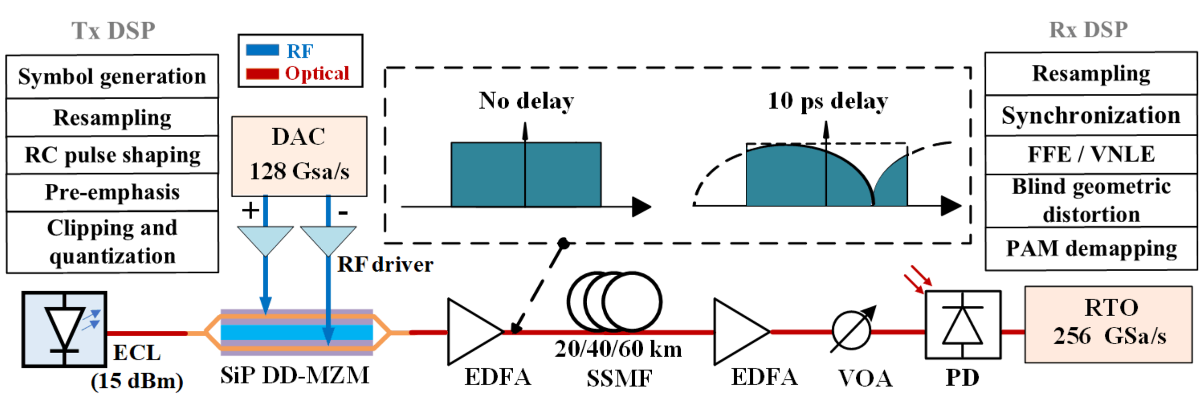

Fig. 2: The experimental setup and the DSP routine employed at the transmitter (Tx) and receiver (Rx). The inset illustrates the impact of the optical delay line on the optical spectrum after the DD-MZM

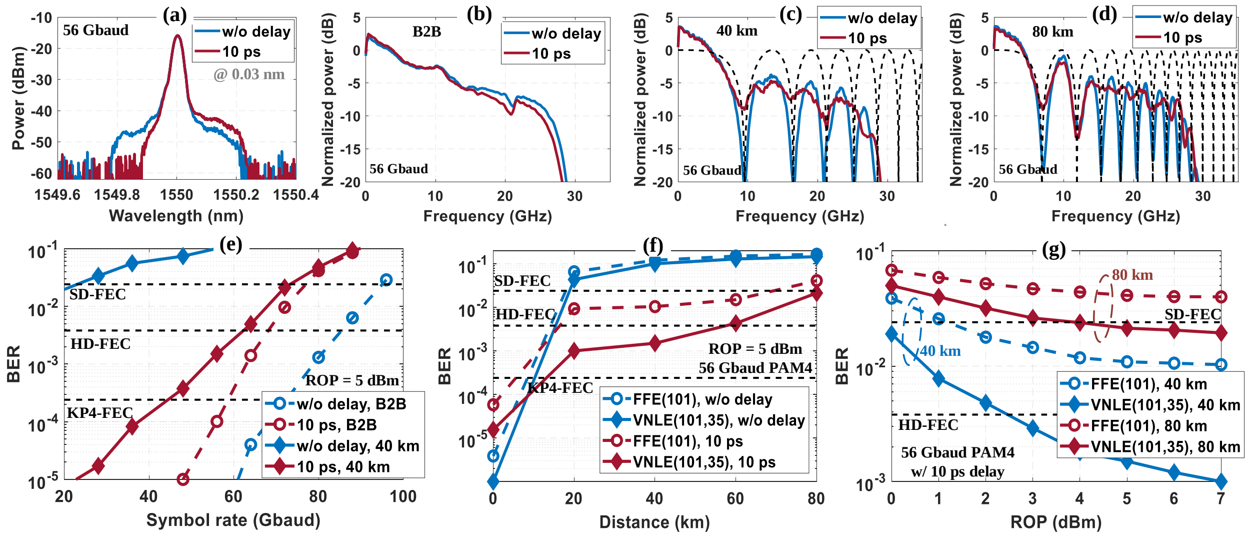

Fig. 3: (a) Optical spectra of the DD-MZM without (w/o) delay and the DD-MZM with 10 ps optical delay line before fiber transmission. (b-d) Electrical spectra of the received waveform after transmission in SSMF at B2B, 40 km, and 80 km (dashed line shows the theoretical transfer function of dispersive chirp-free IMDD channel). (e) BER versus symbol rate at B2B and 40 km transmission using both DD-MZMs with VNLE. (b) The BER versus transmission distance. (c) BER versus ROP for the DD-MZM with 10 ps delay after 40 and 80 km transmission.

Fig. 3(e) shows the achieved BER versus the symbol rate for both DD-MZM structures at B2B and after 40 km transmission. In the absence of CD (B2B transmission), the skew induced by the optical delay line results in a manageable performance penalty because of high-frequency suppression. This penalty increases with the signal bandwidth (symbol rate). After 40 km transmission, CD-induced power fading significantly deteriorates the transmission performance of the base DD-MZM design (without delay). The DD-MZM with 10 ps delay results in a VSB optical signal that results in acceptable performance, allowing the transmission of 56 Gbaud PAM at a BER of 1.5×10^{-3}, which corresponds to over net 100 Gbps assuming the 6.7% overhead HD-FEC threshold. Beyond 70 Gbaud, the B2B and 40 km curves converge, which highlights the DD-MZM bandwidth limitations. Fig. 3(f) depicts the BER versus the transmission distance for both DD-MZMs with either FFE or VNLE. Even after 80 km, the added delay improves the performance and enables the transmission of 56 Gbaud PAM4 under the 2.4×10^{-2} SD-FEC threshold, which corresponds to a capacity-reach product of 8.96 Tbps×km. The BER sensitivity to the ROP after 40 and 80 km transmission using the DD-MZM with the 10 ps delay is shown in Fig. 3(g). Second-order VNLE with 101 first-order and 35 second-order kernels improves the performance considerably compared to linear FFE because of the ripply distorted spectrum of the signal. The gain of employing VNLE is less pronounced after 80 km transmission because of the increase in the number of frequency dips, as shown in Fig. 3(b-d).

The presented DD-MZM with a passive optical delay line adds neither complexity nor cost to the transmission system. Compared to inducing the delay in the RF domain, the proposed structure is advantageous as optical delay lines are compact, costless, and not limited by RF signal bandwidth. Moreover, the demonstrated VSB transmitter uses a single DAC without optical filtering. This work employs conventional DSP, which glorifies the impact of the added passive optical delay line and achieved transmission performance.

4. Conclusion

In summary, we demonstrate a SiP cost-effective VSB transmitter based on a DD-MZM and a passive on-chip optical delay line, which requires a Single DAC without optical filtering. This VSB transmitter enables the transmission of 56 Gbaud PAM4 (line rate 112 Gbps) over 40 and 80 km of dispersion-uncompensated SSMF under the 6.7% HD-FEC and 20% SD-FEC BER thresholds, which respectively correspond to net rates of 105 and 93 Gbps.

Acknowledgments The authors would like to thank Ciena for accessing hardware and CMC Microsystems for facilitating chip fabrication.

References

[1] T. Bo *et al.*, "Optical Single-Sideband Transmitters," J. Lightw. Technol., early access (2022).
[2] Y. Zhu *et al.*, "Time skew enabled vestigial sideband modulation for dispersion-tolerant direct–detection transmission," Opt. Lett., **45**, p. 6138-6141 (2020).
[3] M. S. Alam *et al.*, "C-band 4×200 Gbit/s transmission over 40 km of SSMF with an RF delay-assisted WDM-SSB transmitter," OFC 2021, p. W6A.50.
[4] E. Berikaa *et al.*, "2D Constellation Distortion for Subduing Equalization Noise in Bandwidth-Limited IMDD Systems," IEEE Photon. Technol. Lett., **34**, p.267-270 (2022).